

# Analytical assessment of torque and stator currents of an induction motor due to voltage sags

Vijaya Huchche<sup>1</sup>, Nita Patne<sup>2</sup>

<sup>1</sup>Department of Electrical Engineering, Shri Ramdeobaba College of Engineering and Management, Rashtrasant Tukdoji Maharaj University, Nagpur, India

<sup>2</sup>Department of Electrical Engineering, Visvesaraya National Institute of Technology, Nagpur, India

## Article Info

### Article history:

Received Jun 3, 2022

Revised Oct 6, 2022

Accepted Oct 13, 2022

### Keywords:

Induction motor

Positive and negative sequence torques

Power quality

Symmetrical and

unsymmetrical voltage sag

Symmetrical component theory

## ABSTRACT

Voltage sag is a frequently encountered phenomenon in a power system to which many three phase induction motors are directly connected. This paper presents a simple analytical method for calculation of net electro-magnetic torque and stator currents of an induction motor subjected to symmetrical as well as unsymmetrical sags in supply voltage. This work presents an innovative path to compute net electro-magnetic torque and increase in stator currents for all seven types of sags using the well-known symmetrical component theory. Such a simple method and expressions used in this paper are not reported in the literature reviewed so far. The computation is further extended for different load conditions while varying the symmetrical sag magnitude. The simplicity of analytical assessment of loading effect on electro-magnetic torque from no-load to full-load condition for all sag types is presented. The outcome of the study was verified by imitating the environments for various types of sag in MATLAB/Simulink. The observations are that the average output torque of a motor decreases and ripple in power increases during unsymmetrical sags.

This is an open access article under the [CC BY-SA](https://creativecommons.org/licenses/by-sa/4.0/) license.



## Corresponding Author:

Vijaya Huchche

Department of Electrical Engineering, Shri Ramdeobaba College of Engineering and Management, Rashtrasant Tukdoji Maharaj University

Katol Road, Nagpur-440010, Maharashtra, India

Email: huchchev@rkneec.edu

## 1. INTRODUCTION

Performance of electric machines and power systems is adversely affected by poor power quality. Voltage sag is a dominant factor for poor performance of the industrial equipments [1]. Voltage sag is a short duration reduction in the root mean square (RMS) voltage between 0.1 to 0.9 p.u. at the power frequency which lasts from 0.5 cycles to one minute [2]. It is distinguished by remaining voltage, period, phase angle shift, and the type of faults. A three-phase short circuit results in symmetrical sags, whereas single-line-to-ground, phase-to-phase or two-phase to ground faults results in unsymmetrical sags [2]–[8]. Since voltage sag recovers at the fault current zeros, it amounts to a discrete voltage recovery, Rolan *et al.* [8] divided discrete sags into fourteen types. However, Bollen put forward mainly seven types of voltage sags as experienced at the terminals of equipment [2]. In the present study seven types of sags are considered as per Bollen classification. The detrimental effect of voltage sags on several sensitive equipments in the power system is a point of concern for the researchers. Breakdown of electric motors owing to the voltage sags is a serious problem in the industry. This is also associated with significant monetary loss [9]–[11]. Many studies have explored the effects of voltage sag on the functioning of an induction motor [12]–[18]. Most of the studies mentioned in above references used simulation approach for demonstrating at the most one or two of

the above-mentioned ill effects on induction motors. Very few studies, however, make use of basic analytical methods to study one or two of the above-mentioned ill effects on induction motors exclusively [13], [19], [20]. Corcoles and Pedra [13] proposed an algorithm for the computation of the transient-specifically, current and torque peak and speed loss resulted by a voltage sag in the induction motor supply system. Aung and Milanovic [19], presented the numerical approach to find the dynamic changes of voltage sags on an induction motor. Unsymmetrical (type B only) types of sags were used in the study. Wang *et al.* [20], proposed an analytical method for computation of the critical voltage sag clearance period of induction motors. Sethupathi and Senthilnathan [21] presented speed-time characteristics under full load condition.

A unique feature of the present study was the use of a symmetrical component theory to compute net electro-magnetic torque and the increase in stator currents for all seven types of sags which was not reported earlier. The analytical assessment of loading effect on electro-magnetic torque from no-load to full-load condition for all sag types is presented. The computation was further extended for different load conditions while varying the symmetrical sag magnitude. The system of analysis to get the net electro-magnetic torque and the stator currents through symmetrical and unsymmetrical voltage sags is presented in section 2. Using symmetrical component theory, four case studies are elaborated in section 3. Analytical results in section 3 are qualitatively checked by MATLAB/Simulink in section 4 and the work is summarized in section 5.

## 2. ANALYTICAL ASSESSMENT OF TORQUE AND STATOR CURRENTS

### 2.1. Sequence torque calculations

The supply voltage develops unbalance due to unsymmetrical sag. Positive and negative sequence equivalent circuits were used to calculate sequence torque during sag. A three-phase unbalance voltage set ( $V_a$ ,  $V_b$ , and  $V_c$ ) can be determined into three phase balanced positive sequence ( $V_1$ ), negative sequence ( $V_2$ ), and zero sequence ( $V_0$ ) voltages via symmetrical component theory as presented in (1) to (3) [22].

$$V_1 = \frac{1}{3}(V_a + \alpha V_b + \alpha^2 V_c) \quad (1)$$

$$V_2 = \frac{1}{3}(V_a + \alpha^2 V_b + \alpha V_c) \quad (2)$$

$$V_0 = \frac{1}{3}(V_a + V_b + V_c) \quad (3)$$

where  $\alpha = e^{j120}$ . Using sequence voltages, the voltage unbalance factor (VUF) during sag is determined using (4).

$$\%VUF = \frac{V_2}{V_1} \times 100 \quad (4)$$

Electro-magnetic torque and stator currents are calculated for positive and negative sequence voltages independently. Positive sequence voltage produces an air-gap flux wave, which rotates at synchronous speed in the forward direction. Subjecting a positive sequence equivalent circuit with positive sequence voltage positive sequence stator current ( $I_p$ ) and positive sequence torque ( $T_p$ ) is obtained using (5) and (6) [23].

$$I_p = \frac{V_1}{\left(R_s + \frac{R_r}{s}\right) + j(X_s + X_r)} \quad (5)$$

$$T_p = \frac{3}{\omega_s} \left[ \frac{V_1^2 R_r / s}{\left(R_s + \frac{R_r}{s}\right) + j(X_s + X_r)} \right] \quad (6)$$

Negative sequence voltage produces an air-gap flux wave, which rotates at synchronous speed in the reverse direction. When negative sequence voltage is applied to the negative sequence equivalent circuit, the stator current ( $I_n$ ) and torque ( $T_n$ ) is obtained using (7) and (8) respectively [23].

$$I_n = \frac{V_2}{\left(R_s + \frac{R_r}{2-s}\right) + j(X_s + X_r)} \quad (7)$$

$$T_n = -\frac{3}{\omega_s} \left[ \frac{V_2^2 R_r / (2-s)}{\left(R_s + \frac{R_r}{2-s}\right) + j(X_s + X_r)} \right] \quad (8)$$

The negative sequence current reduces the overall torque [22], [23]. The overall electro-magnetic torque is hence computed using (9).

$$T_e = T_p + T_n \tag{9}$$

Drop in torque operates induction motor at a point determined by the intersection of motor torque-speed curve during sag and load torque characteristics as shown in Figure 1. Basis the change at the operating point, the motor speed reduces from its nominal speed ( $\omega_m$ ) to that at the end of sags ( $\omega'_m$ ). In Figure 1, the  $T_{M-Con}$  curve is of the constant load characteristics; the  $T_{E-pre}$  is the motor's electromagnetic torque curve developed before sag and  $T_{E-sag}$  curve is the reduction in electromagnetic torque due to voltage sag.

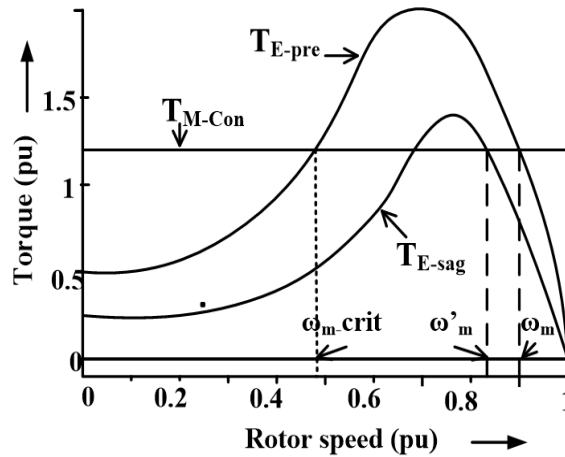


Figure 1. Torque-speed curves for normal and sag voltages

A large unbalance in motor current is encountered due to a small negative sequence impedance relative to positive sequence impedance. Current unbalance factor (CUF) is the ratio of negative sequence current ( $I_n$ ) to positive sequence current ( $I_p$ ) as given in (10).

$$\%CUF = \frac{I_n}{I_p} \times 100 \tag{10}$$

The three phase stator currents during unsymmetrical sags can be found using (11) to (13).

$$I_a = I_p + I_n \tag{11}$$

$$I_b = \alpha I_p + \alpha^2 I_n \tag{12}$$

$$I_c = \alpha^2 I_p + \alpha I_n \tag{13}$$

where  $I_a, I_b, I_c$  are the stator currents in phases  $a, b,$  and  $c$  respectively.

### 3. CASE STUDIES

A 3-HP, 415 V, 50 Hz, 4-pole, squirrel cage delta connected motor having electrical parameters as shown in Table 1 [23] is considered. Three phase voltages for seven types of sags are considered as in Table 2 [2]. Following cases (case 1 to case 4) are studied to calculate net electro-magnetic torque and the stator currents during various voltage sags.

Table 1. Electrical parameters of 3-ph induction motor

$T_L$ (Nm)	$R_s$ ( $\Omega$ )	$R_r$ ( $\Omega$ )	$X_s$ ( $\Omega$ )	$X_r$ ( $\Omega$ )	$X_m$ ( $\Omega$ )	$J$ ( $\text{Kg/m}^2$ )	Pole
11.9	0.435	0.816	0.754	0.754	26.13	0.089	4

Table 2. Characteristics of voltage sags

Sags	Phase A Volts (p.u.)	Phase B Volts (p.u.)	Phase C Volts (p.u.)
A	$0.6\angle 0^\circ$	$0.6\angle -120^\circ$	$0.6\angle -120^\circ$
B	$0.6\angle 0^\circ$	$1\angle -120^\circ$	$1\angle -120^\circ$
C	$1\angle 0^\circ$	$0.72\angle -133.9^\circ$	$0.72\angle -133.9^\circ$
D	$0.6\angle 0^\circ$	$0.92\angle -109.1^\circ$	$0.92\angle -109.1^\circ$
E	$1\angle 0^\circ$	$0.92\angle -120^\circ$	$0.92\angle -120^\circ$
F	$V\angle 0^\circ$	$0.808\angle -111.79^\circ$	$0.808\angle -111.79^\circ$
G	$0.86\angle 0^\circ$	$0.6\angle -129.83^\circ$	$0.6\angle -129.83^\circ$

### 3.1. Case 1: study under balanced voltage condition

When balanced supply voltages as in (14) are applied to the induction motor, the net electro-magnetic torque and the stator currents obtained are as given in (15) and (16) respectively.

$$V_a=239.6\angle 0^\circ; V_b=239.6\angle -120^\circ; v_c=239.6\angle -120^\circ \quad (14)$$

$$T = 35.55 \text{ Nm} \quad (15)$$

$$I_a = 5.9659 \text{ Amp}; I_b = 5.9659\angle -120^\circ \text{ Amp}; I_c = 5.9659\angle 120^\circ \text{ Amp} \quad (16)$$

### 3.2. Case 2: study under unsymmetrical sag type D

Subjecting the induction motor with voltages as in (17) to the unsymmetrical sag type D, positive sequence  $V_1$ , negative sequence  $V_2$  and zero sequence  $V_0$  voltages are calculated using (1) to (3) and values are mentioned as per (18).

$$V_a = 143.76\angle 0^\circ, V_b = 220.43\angle 109.1^\circ, V_c = 220.43\angle 109.1^\circ \text{ volts} \quad (17)$$

$$V_1 = 192.22 \text{ volts}, V_2 = 48.296 \text{ volts}, V_0 = 0.166 \text{ volts} \quad (18)$$

Using (4), voltage unbalance factor is computed as, VUF=25.12%. With slip  $s=0.03$ , positive sequence current and negative sequence currents are calculated using (5) and (7) respectively. The values are given in Table 3. Using (10), current unbalanced factor is calculated as, CUF=466.39%. Using (11 to 13), the three phase stator currents of an induction motor are calculated. The values are given in in Table 3.

Positive sequence torque is calculated using (6) as,  $T_p = 25.0586 \text{ Nm}$ . Negative sequence torque is computed employing (8) as,  $T_n = -6.159 \text{ Nm}$ . The net torque is computed employing (9) as,  $T = 18.899 \text{ Nm}$ . Other sag types were subjected to this method and the output net torques and stator currents are presented in Table 3.

Table 3. Analytical assessment of net torque and stator currents during sag

Type	$V_1$	$V_2$	VUF	$I_1$	$I_2$	CUF	$I_a$	$I_b$	$I_c$	$T_1$	$T_2$	T Nm
A	143.8	-	-	5.19	-	-	$5.19\angle 0^\circ$	$5.19\angle -120^\circ$	$5.19\angle 120^\circ$	25.1	-	25.06
B	207.6	31.94	15.4	7.50	19.53	260.3	$27.03\angle 0^\circ$	$17.06\angle -142^\circ$	$17.06\angle 142^\circ$	29.3	2.698	26.55
C	191.5	47.97	25.1	6.92	29.33	423.8	$36.25\angle 0^\circ$	$26.55\angle -133^\circ$	$26.55\angle 133^\circ$	24.9	6.078	18.79
D	192.2	48.29	25.1	6.95	29.52	425.0	$36.46\angle 0^\circ$	$26.73\angle -133^\circ$	$26.73\angle 133^\circ$	25.1	6.159	18.80
E	175.7	31.95	18.2	6.35	19.53	307.6	$25.88\angle 0^\circ$	$17.25\angle -138.5^\circ$	$17.25\angle 138.5^\circ$	20.94	2.696	18.24
F	175.7	31.84	18.2	6.35	19.46	306.5	$25.81\angle 0^\circ$	$17.19\angle -138.6^\circ$	$17.19\angle 138.6^\circ$	20.94	2.677	18.25
G	163.6	36.20	22.2	5.91	22.13	374.2	$28.04\angle 0^\circ$	$19.84\angle -135^\circ$	$19.84\angle 135^\circ$	18.2	3.461	14.71

### 3.3. Case 3: effect of load on electro-magnetic torque of the induction motor for seven sag types

The torque of an induction motor reduces when it is subjected to voltage sags. Here using symmetrical component theory, the net electro-magnetic torque of an induction motor for different load condition was computed. Load was increased in a step of 10% of full load. Figure 2 shows variation of net

electro-magnetic torque for various loading conditions for all sag types. From this study following results were observed: During light load condition for unsymmetrical sag types (C, D, E, F, and G), negative sequence torque is more than positive sequence torque and hence net electro-magnetic torque of the motor is negative whereas in sag B, negative sequence component is less, therefore net electro-magnetic torque is more as compared to other types of sags from no load to full load conditions.

### 3.4. Case 4: effect of sag magnitude on net electro-magnetic torque of symmetrical sag (sag A) for no load to full load condition

Electro-magnetic torque was computed for different load conditions while simultaneously varying the symmetrical sag magnitudes. Calculations were carried out for variation of sag magnitude by increasing the sag in a step of 20 per cent of supply voltage. Simultaneously load was increased in a step of 10% of full load. Figure 3 shows variation of net electro-magnetic torque Vs percent of full load slip for different magnitudes of symmetrical sag from no load to full load conditions. The net electro-magnetic torque reduces steeply as sag magnitude increases owing to the fact that the reduction in torque is proportional to the square of sag voltage. In case of severe sags, the maximum torque produced can be lower than the load torque as shown in Figure 1. There, the motor speed drops continuously for sag duration triggering the sensitive protection device to turn off the load. In order to prevent stalling of the motor, it is essential to clear the sag before the motor falls to the minimum critical speed. This method of computation is helpful in tuning the motor contactors to protect load assembly. This may help in reducing unwanted stalling of motors. The computation of the net torque as shown in Figures 2 and 3 enables to visualize the dynamic behavior of an induction motor during voltage sag.

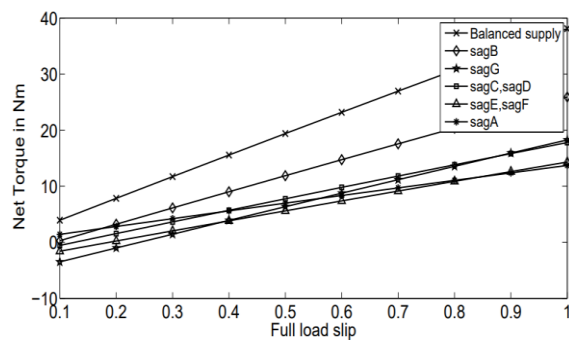


Figure 2. Net torque vs. percent of full load slip for different sags

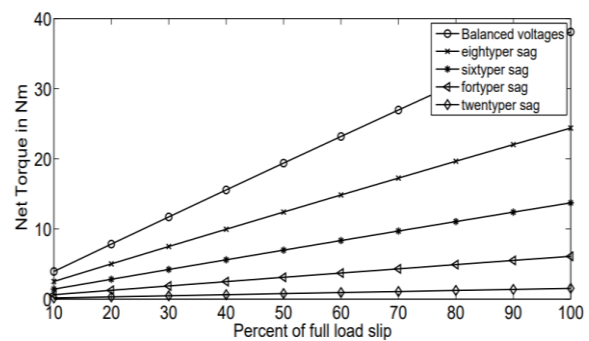


Figure 3. Net torque Vs percent of full load slip for sag

## 4. SIMULATION RESULTS

To verify the responses of different types of sags employing simulation, a 3-phase, 3-HP squirrel cage motor used in analytical assessment was modeled in MATLAB/Simulink [23], [24]. It is critical to identify the characteristics of voltage sags viz. their magnitude, duration, and phase angle variations for studying its effects [25]. A sag generator is assembled in MATLAB/Simulink using embedded MATLAB function. With the help of MATLAB code, seven types of sags were created according to Bollen classification with parameters shown in Table 2. Further, this voltage sag generator can be used for the designing the immunity and sensitivity characteristics. These characteristics help to identify the effect of sags on the motor qualitatively and quantitatively. Figure 4 shows the system, modelled in MATLAB/Simulink for simulation.

When the motor encounters these sag types (Sag-A, Sag-B, Sag-C, Sag-D, Sag-E, Sag-F, and Sag-G), the simulated results of terminal voltage, stator currents, the net electro-magnetic torque, and speed of an induction motor are as shown in Figures 5(a) and (b), Figure 6(a) and (b), and Figure 7(a) to (c). During sags, reduction in electro-magnetic torque and the speed and increase in the stator currents were found for all sag types. Though the unbalance in voltage is small, large unbalance in motor current is observed during unsymmetrical sags owing to the fact that negative sequence impedance of a motor is small as compared to positive sequence impedance [16]. The average output torque of the motor decreases and ripple increases significantly as a consequence of the unbalanced voltages during unsymmetrical sags. In addition, the torque and speed pulsations have a frequency twice that of the power supply as observed in simulation results.

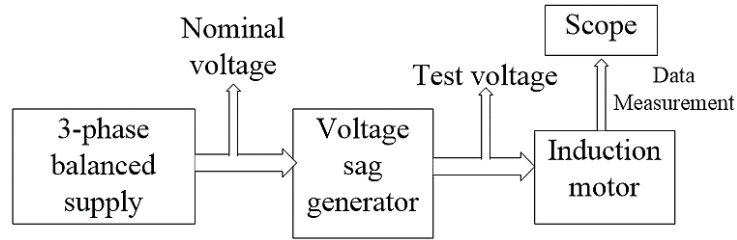


Figure 4. System in MATLAB/Simulink for simulation

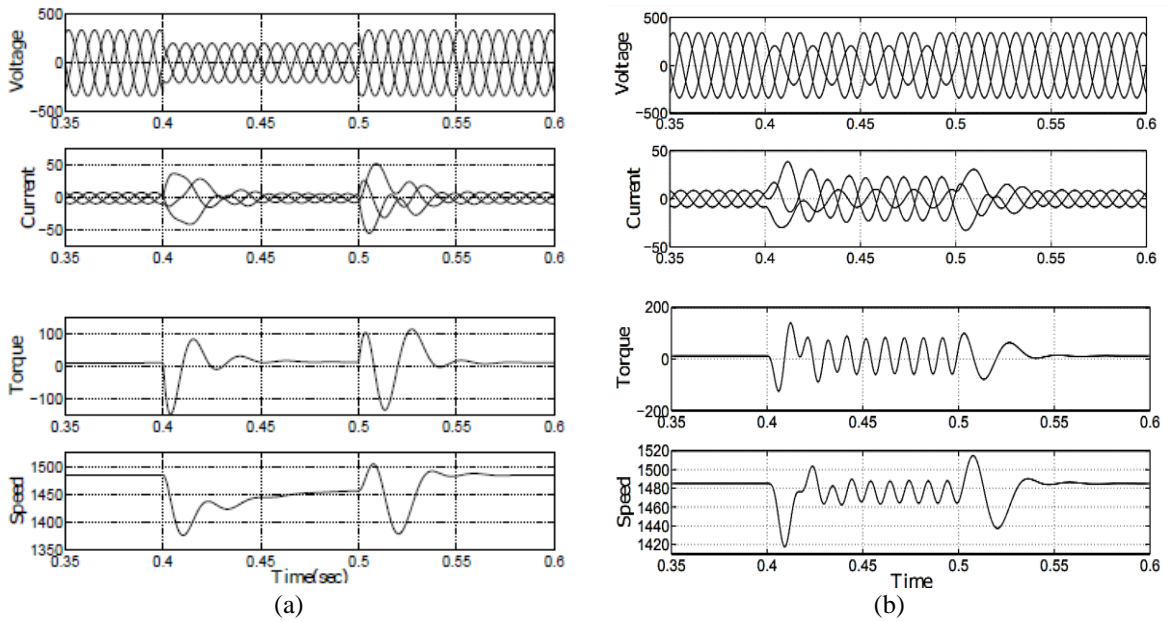


Figure 5. Characteristics of (a) Sag-A and (b) Sag-B

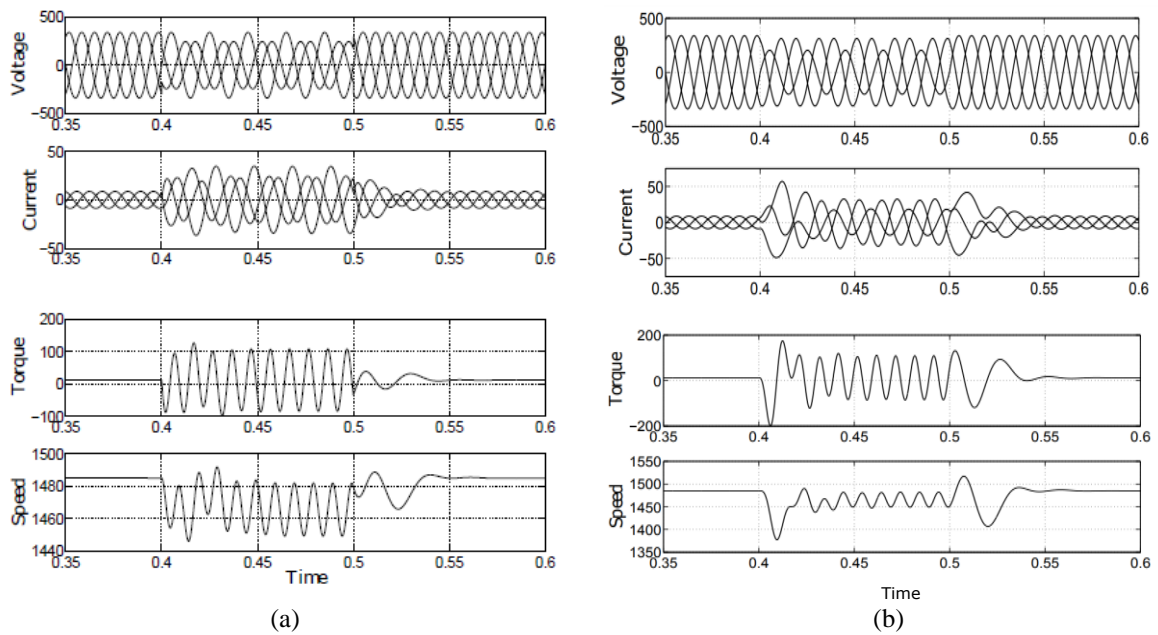


Figure 6. Characteristics of (a) Sag-C and (b) Sag-D

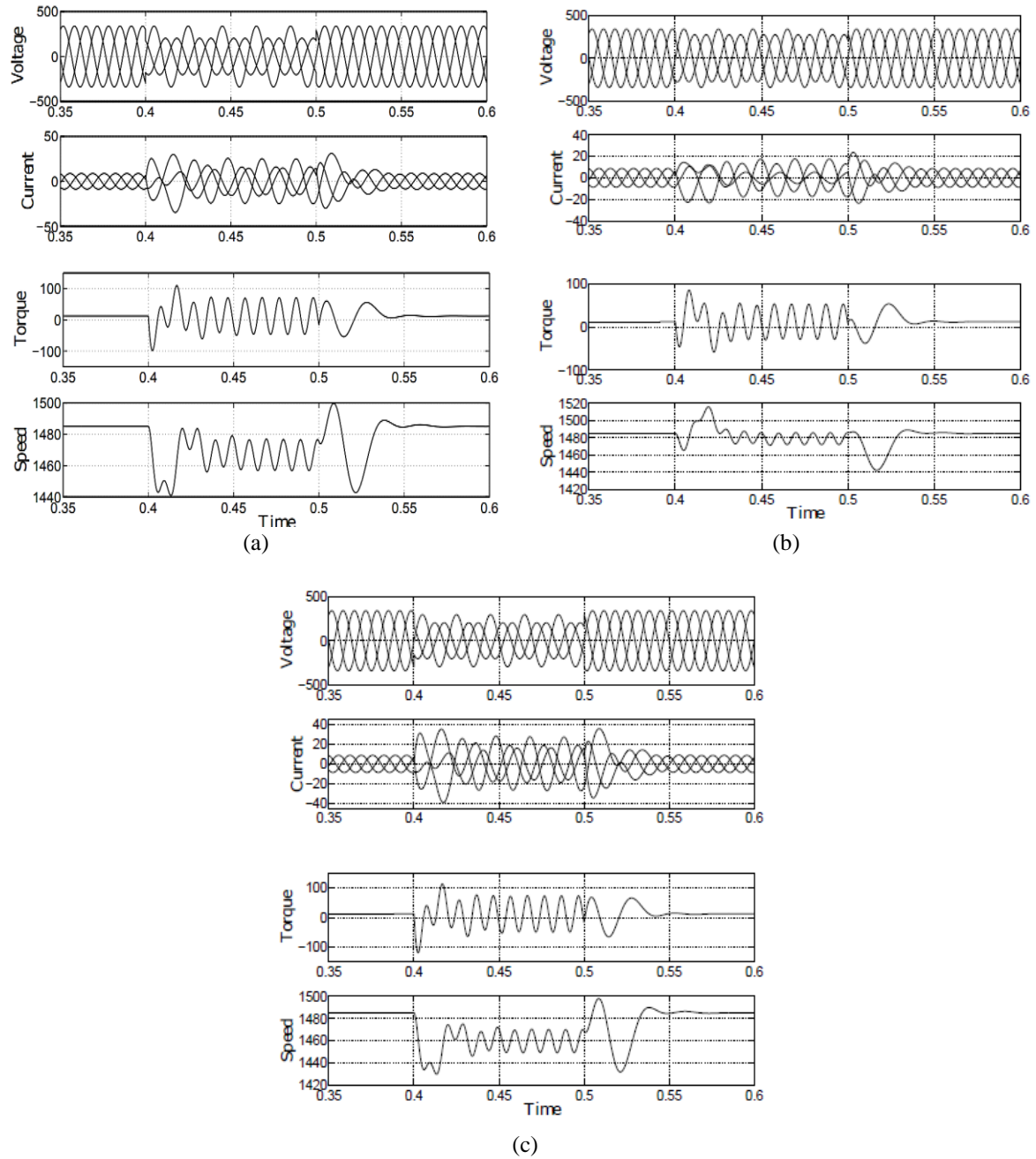


Figure 7. Characteristics of (a) Sag-E, (b) Sag-F, and (c) Sag-G

### 5. CONCLUSION

In this work, a unique method is proposed to compute net electro-magnetic torque and the stator currents of an induction motor during all seven types of sags. The ease of computation is explained in section 2. One of the characteristics of this technique is that, it can also measure electro-magnetic torque for different load conditions while simultaneously varying the symmetrical sag magnitudes. From this study (case3), it is observed that different unsymmetrical sags having identical positive sequence voltage produce identical effects on sags (sag C and D; and sag E and F). During light load condition for sag type C, D, E, F, and G negative sequence torque is more than positive sequence torque and hence net torque of the motor is negative whereas in sag B, negative sequence component is less, therefore net torque for sag B is more compared to the other types of sags from no load to full load conditions. Since reduction in torque is proportional to the square of sag voltage, the net electro-magnetic torque reduces steeply as sag magnitude increases (case 4). In case of severe sags, the maximum torque produced can be lower than the load torque. There, the motor speed drops continuously for sag duration. A voltage sag generator is developed in





MATLAB/Simulink using embedded MATLAB function. With the help of MATLAB code, seven types of sags were created according to Bollen classification. Reduction in torque and hence change in operating point obtained for different sag magnitudes and loading conditions using simulation. But the calculations here are more accurate and are faster. Going further, voltage sag generator and the simulated results of the present study can be substantiated by implementing into the hardware part.

## REFERENCES





- [1] J. Yadav, K. Vasudevan, D. Kumar, and P. Shanmugam, "Power quality assessment for an industrial plant," in *2018 IEEE International Conference on Power Electronics, Drives and Energy Systems (PEDES)*, Dec. 2018, pp. 1–6, doi: 10.1109/PEDES.2018.8707496.
- [2] M. H. Bollen, "Understanding power quality problems: voltage sags and interruptions," *Choice Reviews Online*, vol. 37, no. 8, Apr. 2000, doi: 10.5860/CHOICE.37-4522.
- [3] M. H. J. Bollen, "Voltage recovery after unbalanced and balanced voltage dips in three-phase systems," *IEEE Transactions on Power Delivery*, vol. 18, no. 4, pp. 1376–1381, Oct. 2003, doi: 10.1109/TPWRD.2003.817725.
- [4] M. S. Hasan, K. M. Muttaqi, and A. Bouzardoum, "Characterization of voltage sag based on point-on-wave," in *2016 9th International Conference on Electrical and Computer Engineering (ICECE)*, Dec. 2016, pp. 259–262, doi: 10.1109/ICECE.2016.7853905.
- [5] P. Wei, Y. Xu, and Q. Lan, "Voltage sag classification with consideration of phase shift," in *2017 IEEE International Conference on Energy Internet (ICEI)*, Apr. 2017, pp. 159–164, doi: 10.1109/ICEI.2017.35.
- [6] Y. Han, Y. Feng, P. Yang, L. Xu, Y. Xu, and F. Blaabjerg, "Cause, classification of voltage sag, and voltage sag emulators and applications: a comprehensive overview," *IEEE Access*, vol. 8, pp. 1922–1934, 2020, doi: 10.1109/ACCESS.2019.2958965.
- [7] P. B. Bandla, I. Vairavasundaram, Y. Teekaraman, R. Kuppasamy, and S. Nikolovski, "Real time sustainable power quality analysis of non-linear load under symmetrical conditions," *Energies*, vol. 15, no. 1, Dec. 2021, doi: 10.3390/en15010057.
- [8] A. Rolán, F. Córcoles, J. Pedra, L. Monjo, and S. Bogarra, "Testing of three-phase equipment under voltage sags," *IET Electric Power Applications*, vol. 9, no. 4, pp. 287–296, Apr. 2015, doi: 10.1049/iet-epa.2014.0258.
- [9] J. Y. Chan and J. V. Milanovic, "Methodology for assessment of financial losses due to voltage sags and short interruptions," in *2007 9th International Conference on Electrical Power Quality and Utilisation*, Oct. 2007, pp. 1–6, doi: 10.1109/EPQU.2007.4424119.
- [10] N. R. Patne and K. L. Thakre, "Effect of transformer type on estimation of financial loss due to voltage sag-PSCAD/EMTDC simulation study," *IET Generation, Transmission and Distribution*, vol. 4, no. 1, 2010, doi: 10.1049/iet-gtd.2008.0500.
- [11] Y. C. Jhan, J. V. Milanović, and A. Delahunty, "Risk-based assessment of financial losses due to voltage sag," *IEEE Transactions on Power Delivery*, vol. 26, no. 2, pp. 492–500, Apr. 2011, doi: 10.1109/TPWRD.2009.2037426.
- [12] J. Pedra, F. Córcoles, and L. Sainz, "Effects of unsymmetrical voltage sags on squirrel-cage induction motors," *IET Generation, Transmission and Distribution*, vol. 1, no. 5, 2007, doi: 10.1049/iet-gtd:20060555.
- [13] F. Corcoles and J. Pedra, "Algorithm for the study of voltage sags on induction machines," *IEEE Transactions on Energy Conversion*, vol. 14, no. 4, pp. 959–968, 1999, doi: 10.1109/60.815014.
- [14] M. Petronijević, B. Veselić, N. Mitrović, V. Kostić, and B. Jeftenić, "Comparative study of unsymmetrical voltage sag effects on adjustable speed induction motor drives," *IET Electric Power Applications*, vol. 5, no. 5, 2011, doi: 10.1049/iet-epa.2010.0144.
- [15] A. Khergade, S. Garg, R. J. Satputaley, and S. Tembhekar, "Analysis of different types of voltage sag and its effects on adjustable speed drive," in *2018 IEEE International Conference on Power Electronics, Drives and Energy Systems (PEDES)*, Dec. 2018, pp. 1–6, doi: 10.1109/PEDES.2018.8707446.
- [16] V. Huchche, N. Patne, and A. Junghare, "Computation of energy loss in an induction motor during unsymmetrical voltage sags-A graphical method," *IEEE Transactions on Industrial Informatics*, vol. 14, no. 5, pp. 2023–2030, May 2018, doi: 10.1109/TII.2017.2763606.
- [17] J. C. Gomez, M. M. Morcos, C. A. Reineri, and G. N. Campetelli, "Behavior of induction motor due to voltage sags and short interruptions," *IEEE Transactions on Power Delivery*, vol. 17, no. 2, pp. 434–440, Apr. 2002, doi: 10.1109/61.997914.
- [18] P. Pillay, P. Hofmann, and M. Manyage, "Derating of induction motors operating with a combination of unbalanced voltages and over or undervoltages," *IEEE Transactions on Energy Conversion*, vol. 17, no. 4, pp. 485–491, Dec. 2002, doi: 10.1109/TEC.2002.805228.
- [19] M. T. Aung and J. V. Milanovic, "Analytical assessment of the effects of voltage sags on induction motor dynamic responses," in *2005 IEEE Russia Power Tech*, Jun. 2005, pp. 1–7, doi: 10.1109/PTC.2005.4524363.
- [20] Z. Wang, X. Wang, and C. Y. Chung, "An analytical method for calculating critical voltage sag clearance time of induction motors," *IEEE Transactions on Power Delivery*, vol. 27, no. 4, pp. 2412–2414, Oct. 2012, doi: 10.1109/TPWRD.2012.2202204.
- [21] P. Sethupathi and N. Senthilnathan, "Comparative analysis of line-start permanent magnet synchronous motor and squirrel cage induction motor under customary power quality indices," *Electrical Engineering*, vol. 102, no. 3, pp. 1339–1349, Sep. 2020, doi: 10.1007/s00202-020-00955-2.
- [22] G. K. Dubey, *Fundamentals of electrical drives*, CRC press, 2002.
- [23] P. C. Krause, O. Wasynczuk, and S. D. Sudhoff, "Analysis of E-machinery and drive systems," WileySons, Inc. *IEEE Publication*, 2002.
- [24] J. Pedra, I. Candela, and L. Sainz, "Modelling of squirrel-cage induction motors for electromagnetic transient programs," *IET Electric Power Applications*, vol. 3, no. 2, 2009, doi: 10.1049/iet-epa:20080043.
- [25] K. Daychosawang and Y. Kumsuwan, "Balanced and unbalanced three-phase voltage sag generator for testing electrical equipment," in *2014 11th International Conference on Electrical Engineering/Electronics, Computer, Telecommunications and Information Technology (ECTI-CON)*, May 2014, pp. 1–6, doi: 10.1109/ECTICon.2014.6839786.



**BIOGRAPHIES OF AUTHORS**

**Vijaya Huchche**     received the B.E. degree in electrical engineering from Marathwada University, Aurangabad, India, in 1992; the M.Tech. degree in integrated power systems in 2002 and the Ph.D. degree in electrical engineering in 2017 from Visvesvaraya National Institute of Technology, Nagpur, India. She is currently an Assistant Professor at the Electrical Engineering Department, Shri Ramdeobaba College of Engineering and Management, Nagpur, India. Her research interests are in Electrical machines, Power quality, Applications of power electronics in power systems, Fuzzy logic and its applications, DC micro-grid. She can be contacted at email: huchchev@rknc.edu.



**Nita Patne**     received the B.E. degree in electrical engineering from Amravati University, Amravati, India, in 1993; the M.Tech. degree in integrated power systems in 2001; and the Ph.D. degree in electrical engineering in 2010 from Visvesvaraya National Institute of Technology, Nagpur, India. She is currently an associate professor at the Electrical Engineering Department, Visvesvaraya National Institute of Technology, Nagpur, India. Her research interests are in smart grid, power quality, power system protection and application of power electronics in power systems. She can be contacted at email: nrpatne@eee.vnit.ac.in.